PNAS Nexus, 2026, **5**, pgag211
https://doi.org/10.1093/pnasnexus/pgag211
Published: 7 July 2026
Biological, Health, and Medical Sciences

A train-and-assist device that upskills novices to strengthen the workforce and expand diagnostic access

Minkyo Lee[1], Xinyue (Penny) Pei[2], Si Hyung Jin[2], Natasha Shelby[2], Rani Gera[3], Alexander Viloria Winnett[2], Colin F. Camerer[3], Mahbubur Rahman[4], Nils Pilotte[5], Steven A. Williams[6,7], and Rustem F. Ismagilov[1,2,8]*

[1]Andrew and Peggy Cherng Department of Medical Engineering, Division of Engineering and Applied Science, California Institute of Technology, Pasadena, CA 91125, USA
[2]Division of Chemistry and Chemical Engineering, California Institute of Technology, Pasadena, CA 91125, USA
[3]Division of the Humanities and Social Sciences, California Institute of Technology, Pasadena, CA 91125, USA
[4]Environmental Health and WASH, Health Systems and Population Studies Division, International Centre for Diarrhoeal Disease Research, Bangladesh (icddr, b), Dhaka 1212, Bangladesh
[5]Department of Biological Sciences, Quinnipiac University, Hamden, CT 06518, USA
[6]Department of Biological Sciences, Smith College, Northampton, MA 01063, USA
[7]Molecular and Cellular Biology Program, University of Massachusetts, Amherst, MA 01003, USA
[8]Division of Biology and Biological Engineering, California Institute of Technology, Pasadena, CA 91125, USA
*To whom correspondence should be addressed: Email: rustem.admin@caltech.edu
Edited By David Brenner

Abstract

AI and automation technologies are displacing millions of workers across industries in developed countries, while many developing nations continue to grapple with chronically high unemployment. Meanwhile, healthcare laboratories—particularly in resource-limited settings (including rural and community sites within high-income countries)—face acute shortages of trained staff and the high cost of molecular diagnostics. Here, we propose a "train-and-assist" class of devices that aims to both (i) upskill—rather than replace—workers and (ii) expand diagnostic capacity in a cost-effective way. We describe a device that trains and assists laboratory-inexperienced personnel to perform sample-pooling procedures, which enable high-performance molecular testing at lower costs and higher throughput. A 48-participant user study demonstrated that the device enabled both skill acquisition and high-accuracy pooling. A device-validation study using clinical stool specimens demonstrated that device-assisted pooling agreed 100% with individual assays for soil-transmitted helminths, which affect >1.5 billion people worldwide.

Keywords human–machine interaction, diagnostics, global health, human learning and training, resource-limited settings

Significance statement

While AI and robotic technologies displace workers across industries, healthcare faces labor shortages, especially in diagnostics. We introduce an open-source "train-and-assist" device class that converts this labor surplus into diagnostic capacity. Our first device in this class guides laboratory novice users through complex five-sample-pooling procedure for molecular tests, providing real-time error detection, error correction, and quality control. This study shows that the device eliminated human errors, up-skilled novices, and enabled pooled testing to achieve 100% agreement with individual-sample qPCR for a neglected tropical disease. We aim for our work to spur further innovation in this device class—tools that augment, not replace, the workforce—and to expand diagnostic access for underserved communities, from rural US hospitals to resource-limited clinics worldwide.

Received: November 13, 2025. **Accepted:** June 2, 2026

Introduction

Labor market imbalances present a key challenge in both developing and developed countries. Many developing countries have high unemployment and lack training opportunities. In developed countries, advances in AI and automation are reshaping the labor market across multiple sectors (1, 2), with projections that millions of workers may be displaced by AI within the next decade (2–4). Healthcare, in contrast, has historically suffered from a global shortage of skilled workers in both developing and developed countries, particularly for clinical diagnostic services (5, 6). Persistent vacancies are documented in both low-income regions and high-income countries (HICs), such as the United States (7, 8), Canada (9), and the United Kingdom (10). The reasons for the lack of skilled clinical laboratorians are complex, but two known drivers are the limited training and certification programs and the challenges and burdens associated with entry-level requirements and licensure (7). Although automation and AI will offset some healthcare labor needs (11), they will not offset the growing demand for healthcare services that require skilled workers (1, 2). Specifically, rural hospitals, community pharmacies, and long-term-care facilities remain diagnostically underserved even within wealthy health systems. In both developing and developed countries, the coexistence of surplus labor in some sectors and persistent shortages in diagnostics highlights an urgent need for innovative technologies that can rapidly upskill staff and enable newcomers to perform critical tasks with confidence (Fig. 1a).

Beyond workforce shortages, the diagnostics field has faced another critical challenge: limited access to high-performance testing in resource-limited settings (RLSs) (12). Nucleic acid amplification tests (NAATs) are essential tools to combat high-burden infectious diseases globally, including HIV (13), hepatitis C virus (HCV) (14), tuberculosis (TB) (15), neglected tropical diseases (NTDs) (16–18), and respiratory viruses, such as influenza (19), respiratory syncytial virus (20), and severe acute respiratory syndrome (21). NAATs with high analytical sensitivity and specificity that can be used at the point-of-care (POC) are keys, particularly for underserved populations without access to clinical laboratories (22). POC testing can enable patients to swiftly receive the correct treatment, reducing the risk of being lost to follow-up (23). Yet, despite their high utility, POC NAATs are either unavailable or prohibitively expensive in many contexts—both in HICs (24–26) and in low- and middle-income countries (LMICs) (14, 15, 27). For example, integrated sample-to-answer molecular POC tests exist for HCV RNA, but they are not as widely used as HCV POC antibody tests due to the high cost per test (14).

Sample pooling is a laboratory technique that reduces per-sample diagnostic testing costs and increases the total number of patients that can be tested (28–34). In sample pooling, equal volumes from specimens from different individuals are pooled together and input into a single diagnostic test. Pooling thereby reduces the number of total tests required to be run and subsequent cost for each result. For high-sensitivity POC NAATs, the cost per sample with pooling becomes similar to low-sensitivity POC immunoassays (31, 35–37). Although pooling dilutes individual specimens, high-analytical-sensitivity molecular tests still yield the correct qualitative results for the pools (28–34) and in many cases achieve far superior analytical sensitivity (31, 32, 38) than POC immunoassays (Fig. 1b).

Pooling specimens for use with NAAT diagnostics can enable public health surveillance on a scale that is currently cost prohibitive (33, 34, 39–41). One example is the surveillance for soil-transmitted helminths (STHs), an NTD that affects >1.5 billion people (18). Mass drug administration (MDA) using anti-helminth preventive chemotherapy has reduced disease prevalence; however, to identify when MDA can be stopped (when prevalence of moderate-to-heavy intensity infections is below 2% (18)), large-scale diagnostic testing must be performed (42, 43). Current STH testing is performed by manual DNA extraction followed by qPCR (16, 34); therefore pooling of raw samples upstream of DNA extraction would reduce the cost of and increase the throughput of testing (34). Because most STH-vulnerable regions are in LMICs where testing resources are limited, sample pooling for NAATs could logistically and financially enable testing at the scale needed to inform cessation of MDA (34).

However, the manual sample-pooling process is error prone (29, 32, 33, 44). Skilled personnel must safely handle multiple clinical specimens (33, 44), transfer accurate amounts of samples to each pool (29), avoid cross contamination (32), and maintain documentation (32, 33, 44). Automated liquid handlers for pooling exist (33), but their high cost and a lack of laboratory infrastructure make them infeasible in most RLS (45). Sample pooling is therefore inaccessible in regions where it is most critically needed to expand testing.

Here, we propose a class of technologies that train and assist personnel to learn skills for complex laboratory tasks, with the goal of strengthening the diagnostics workforce and expanding healthcare access. As the initial example of technology in this class, we designed a low-cost, instructional pooling device that assists and trains laboratory-inexperienced personnel to pool clinical specimens for subsequent diagnostic testing (Fig. 1c and Movie S1), which we illustrate with STH testing. We anticipate at least three contexts in which the instructional pooling device would have high impact (i) rapid and widespread molecular diagnostic testing, such as during outbreaks and other testing surges, (ii) manual pooling tasks in RLS where automated equipment such as liquid handlers are cost prohibitive or otherwise impractical, and (iii) programmatic screening/surveillance on a broad scale (such as for disease-elimination efforts).

Pooling was an important strategy to mitigate testing surges during the COVID-19 pandemic (33) but was largely limited to labs that could perform automated pooling, whereas with the instructional device, pooling could be used on a massive scale, even in labs with limited resources and regions with minimally trained personnel. In decentralized RLS (e.g. mobile clinics) that collect specimens, the device is designed to help minimally trained workers perform high-quality, on-site pooling of aliquots with minimal human error. The resulting pooled tubes could be tested locally on POC NAAT platforms (e.g. Cepheid GeneXpert) or using existing manual workflows. In centralized RLS that must process larger numbers of specimens manually for screening/surveillance—as is the case with NTD testing—the device is intended to assist with pooling of primary specimens while automatically logging sample barcodes and pool-quality metrics, significantly increasing the number of results that can be obtained with the manual NAAT workflows.

To evaluate the utility of the device, we conducted a user study with a crossover design to demonstrate device usability and to qualitatively and quantitatively determine the device's assistive (Fig. 1d) and training effects (Fig. 1e) compared with traditional printed (paper) instructions. We also conducted a device-validation study using STH clinical stool samples to demonstrate the utility of the device for pooled molecular testing that would enable public health surveillance of NTDs.

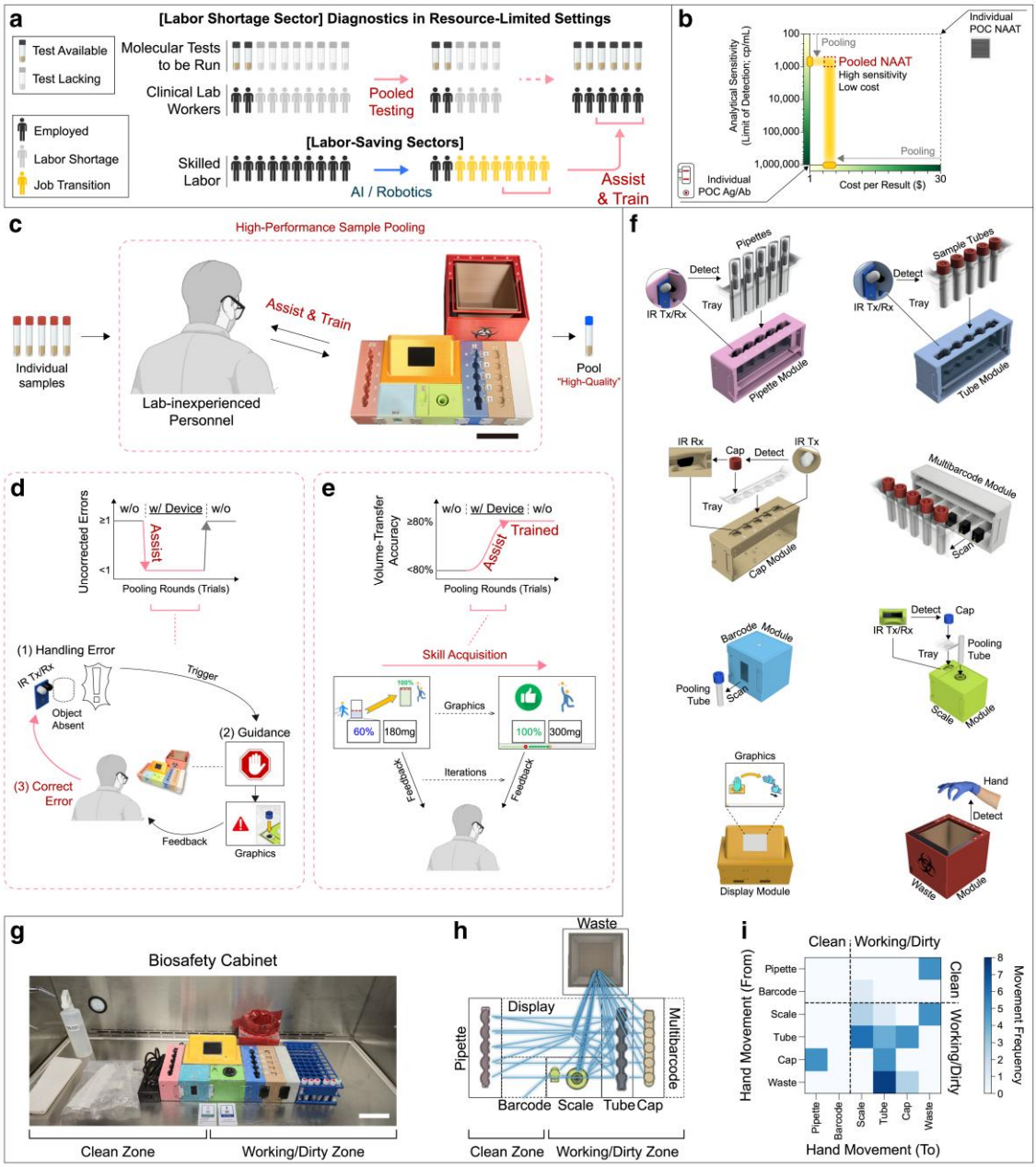

Figure 1 An interactive and instructional device for assisting and training users to perform diagnostic sample pooling. a) Clinical laboratories suffer from shortages of trained workers (top), while other workplace sectors experience reduced labor needs after implementation of advanced technologies (bottom). A novel class of assistive/training technology enabling pooled NAAT would resolve the labor shortage and scale-up high-performance testing in resource-limited settings. b) High-analytical-sensitivity pooled NAATs provide decreased cost-per-result levels comparable to low-analytical-sensitivity POC Ag/Ab tests. c) Instructional device to assist and train laboratory-inexperienced personnel in pooling. Scale bar: 10 cm. d) Device-assistive effect reducing user errors with the use of the device. e) Device-training effect improving volume-transfer skills over multiple pooling iterations. f) Device modules house electronic sensors to monitor the handling workflow. g) Device within a biosafety cabinet alongside materials (e.g. towels, disinfectants, etc.) for clinical sample pooling. Scale bar: 10 cm. h) Expected movement of materials by user (overlaid lines) while using the device. i) Matrix of expected hand movement frequency between two device modules during the pooling. Dashed lines separate clean and working/dirty zones.

Results

Design features of an instructional device for POC pooling

The instructional pooling device is built with open-source embedded systems, interfacing with eight 3D-printed, independently replaceable modules for the application of five-sample pooling (combining five individual samples into a single pool; Fig. 1f). The device modules are equipped with low-cost, off-the-shelf electronic components, including 940 nm infrared diodes for object detection and 640 × 480-resolution barcode scanners for sample identification (Figs. S1 and S2; see Materials and methods for electronic components details), to monitor objects

such as sample tubes, caps, and individually wrapped pipettes (Figs. 1f and S3).

The device layout and step-by-step instructions are designed based on general biosafety protocols for handling clinical samples, with consideration of contamination risk and human factors (Text S1). The layout adopts a left-to-right workflow and separates a clean zone, where nonbiohazardous materials are placed, and a working/dirty zone within a limited space (e.g. biosafety cabinet; Fig. 1g and h). This layout reduces the frequency of hand movement across clean and working/dirty zones, which may help prevent cross contamination and minimize biosafety risks (Fig. 1i).

To enable accurate transfer of sample volumes in RLS where calibrated lab-grade pipettes are not available, the device is designed to work with disposable dual-bulb pipettes that transfer set volumes (this study: 300 µL) of liquid (Fig. S4a). To protect the device against contamination from clinical specimens during the handling workflow, device-protective disposable polypropylene trays manufactured via vacuum-forming technology (Fig. S4b) are placed over certain areas of the device modules.

The device incorporates several user-friendly design features, including colorblind-friendly color-coding and shape-based designs (Fig. S4c). Protective trays have unique shapes that pair exclusively to the corresponding module, similar to shape-sorting blocks (Fig. S4d). The device layout uses intuitive symbolic indicators to guide users through proper pooling procedures (Fig. S4e).

Device functionalities for easy-to-perform POC pooling

The device is designed for deployment in public health laboratories, mobile clinics, or other near-patient settings that routinely use cartridge-based, sample-to-answer NAAT platforms (e.g. Cepheid GeneXpert) or standard benchtop PCR thermocyclers. To make the pooling workflow easy to perform, the device features step-by-step guidance, real-time monitoring of the workflow, and quality-control documentation. Instructional guidance via language-agnostic graphics (Fig. 2a and Text S1) and visual and audible cues is provided by an algorithm (Fig. 2b and Movie S2) at every step. In parallel, the device monitors the user's actions and detects errors in real time through dynamically configured, scenario-based interrupt handlers (Fig. 2c). The device helps users fix correctable mistakes (Fig. 2d, Text S2, and Movie S3); if a detected mistake is uncorrectable, the device will guide the user to terminate the process (Fig. 2b, Text S2, and Movie S4).

Equipped with load cells and strain sensors (Figs. 2e and S5), the device measures the weight of the transferred sample with >98% accuracy and precision (1.94%CV) during volume-transfer steps, when users transfer liquid from individual tubes to the pooling tube using 300-µL dual-bulb pipettes (Fig. 2f). The device measurement shows strong agreement with laboratory-grade analytical balance-based measurements (Pearson's r: 0.983; Fig. 2g). During the volume-transfer activities, the weight values of each transferred sample and the percentages (relative to the target 300 µL) are shown to the user in real time, to reinforce the quality of pooled sample volumes (Fig. 2h). All weight data are paired with tube barcodes and recorded on a removable Secure Digital card in the device, with wireless transmission capability (Figs. 2i and S1).

User study design

We conducted a within-subject user study to evaluate two primary questions: (i) whether an instructional pooling device could assist laboratory-inexperienced personnel in improving their performance when handling challenging sample types, and (ii) whether the device could effectively train these personnel to maintain high-performance levels in sample pooling without the assistance from the device. We enrolled 48 participants, 37 (77%) of whom had limited or no prior laboratory experience (Fig. S6).

Participants were allocated to one of two training protocols (protocols 1 and 2; Tables S1–S5). Protocol 1 was structured to examine the effectiveness of paper instructions in training participants and the subsequent impact of introducing the device. Protocol 2 was designed to investigate the device's effectiveness in improving performance during device use and maintaining performance (skill acquisition) after device removal. In each round of pooling, participants were guided to pool 300 µL of artificial respiratory or stool samples (Fig. S7) with either paper instructions (Text S3) or the device. Each participant completed 16 total rounds of five-sample pooling over two nonconsecutive days ("day 1" and "day 2"; Fig. 3a and b). After the exercises each day, participants evaluated the usability of instructional tools (paper or device) and perceived training effectiveness via questionnaires: poststudy system usability questionnaire (PSSUQ; Tables S6 and S7), Kirkpatrick training evaluation questionnaire (KTEQ; Fig. S8c), and posttraining effectiveness questionnaire (PTEQ; Fig. S8d–f; see Materials and methods for details).

Self-reported surveys: users prefer the instructional device over paper instructions

Protocol 1 participants, who evaluated the usability of paper instructions on day 1 and the device on day 2 (Fig. 3a), reported that both paper and device instructions were useful and provided high information and interface quality (Figs. S8a, b and S9). In contrast, protocol 2 participants, who were exposed to both the paper instructions and the device on day 1 (Fig. 3b), reported that the device was more useful and provided better quality of information and interface than the paper instructions (Figs. 3c, d and S9).

Across both protocols, most users (≥75%) reported strong perceptions of skill acquisition (Likert score ≥4; Fig. S8c) and skill utilization (Fig. S8d and Table S9). Over 90% of users in both protocols also reported perceived knowledge gain (Likert score ≥4; Fig. S8c), although the corresponding result for protocol 1, where users performed paper-assisted pooling over 16 rounds, was statistically less robust (Table S9). Notably, participants felt more confident performing high-performance pooling using the device compared with the paper instructions (Fig. S8e, f and Table S9).

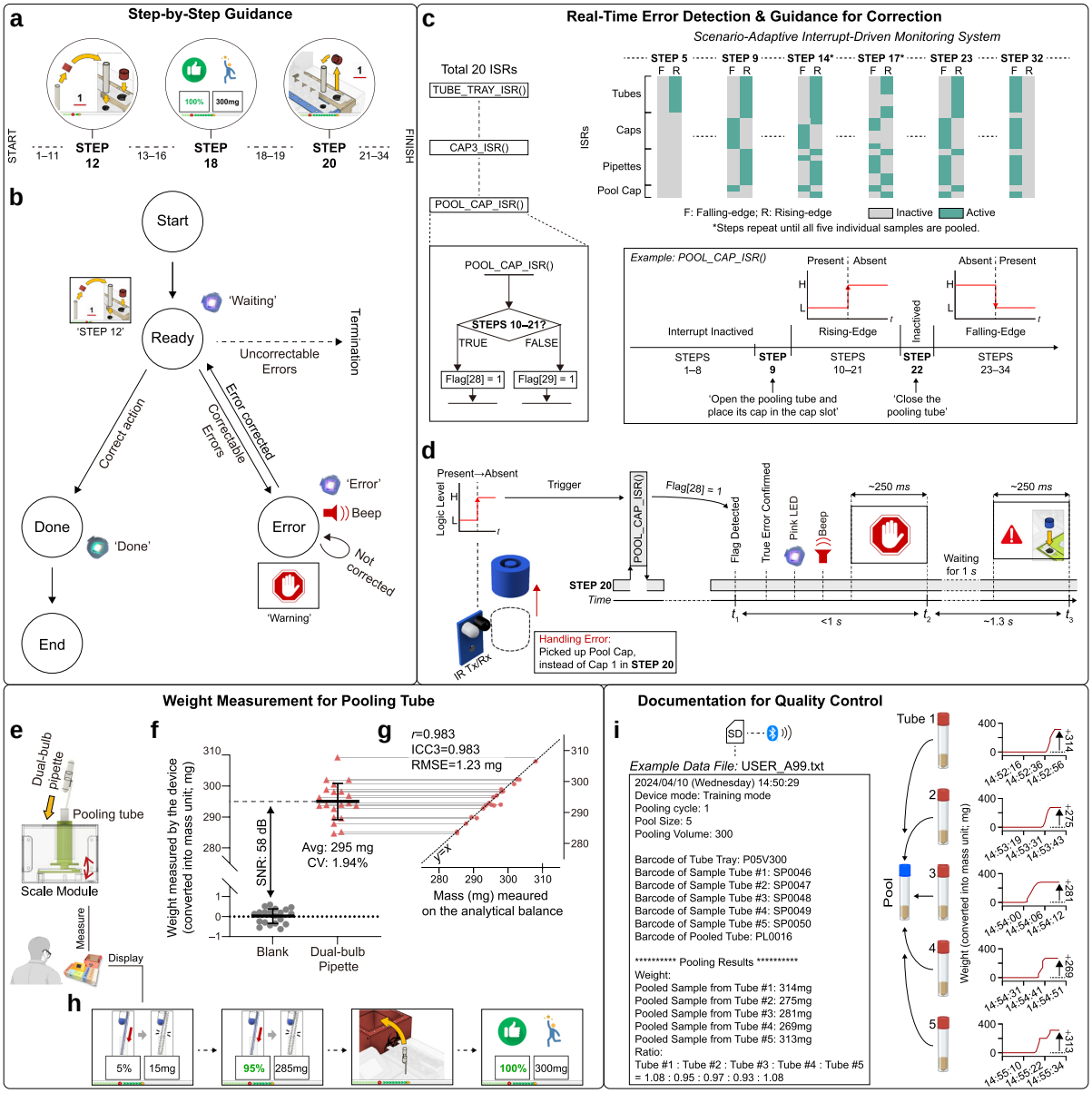

Figure 2 Device functionalities to enable easy-to-perform POC pooling. a) Step-by-step guidance using language-agnostic graphics displayed on the device screen. b) State diagram of the algorithm operated at every guidance step. c) Illustration of scenario-adaptive interrupt-driven system for real-time error monitoring. During the process, the system dynamically reconfigures trigger types between rising and falling edges for 20 interrupt service routines (ISRs). As an example, POOL_CAP_ISR() is inactive until STEP 9 that guides users to open the pooling tube and put its cap into the empty cap slot. During STEPS 10–21, the rising-edge is set to detect errors removing the cap from the slot. After STEP 22, the falling edge is set until the end of process. When executed, the ISR raises a flag, based on scenarios. d) Example process of real-time error detection and correction guidance when a pool cap is removed in STEP 20 which guides to pick up the cap of tube 1. A rising-edge trigger causes the system to immediately pause the workflow and execute POOL_CAP_ISR(). The system detects the raised flag and provides guidance. e) Illustration of the scale module measuring the weight of pooling tube during the volume transfer. f) Scatter plot of weight measured on the device scale before and after the volume transfer ($n = 20$) of 300-μL water. "Blank": the weight on the tared scale; "Dual-bulb pipette": the weight of water transferred by pipettes; Avg, average; CV, coefficient of variation. g) Correlation plot comparing measurements ($n = 20$, dots) between device and laboratory-grade analytical balance. Coefficients r and ICC3 were acquired through Pearson's ($P < 0.00001$) and interclass correlation analyses ($P < 0.00001$). RMSE, root-mean-squared error. h) Real-time feedback of transferred sample amount and percentage on the screen. i) Documentation feature. The example file shows recorded data, including scanned barcodes and the weight of transferred samples. Inlet plots show the weight measurement during the volume transfer.

Protocol 1: assistive effects of the device resulting in improved volume-transfer accuracy and handling error reduction

To investigate assistive effects of the device on sample-handling competency, we analyzed quantitative performance metrics measured during the pooling process in the protocol 1 group. These metrics included the total number of uncorrected handling errors (err_{all}; Text S4), categorized as severe (err_{severe}) and minor (err_{minor}; Table S10), and volume-transfer accuracy (Acc_{pool}). The handling errors were recorded through researcher observation, while scanned barcodes and weight values were recorded via a customized data logger (paper-assisted pooling) or the instructional device (device-assisted pooling; see Materials and methods for details).

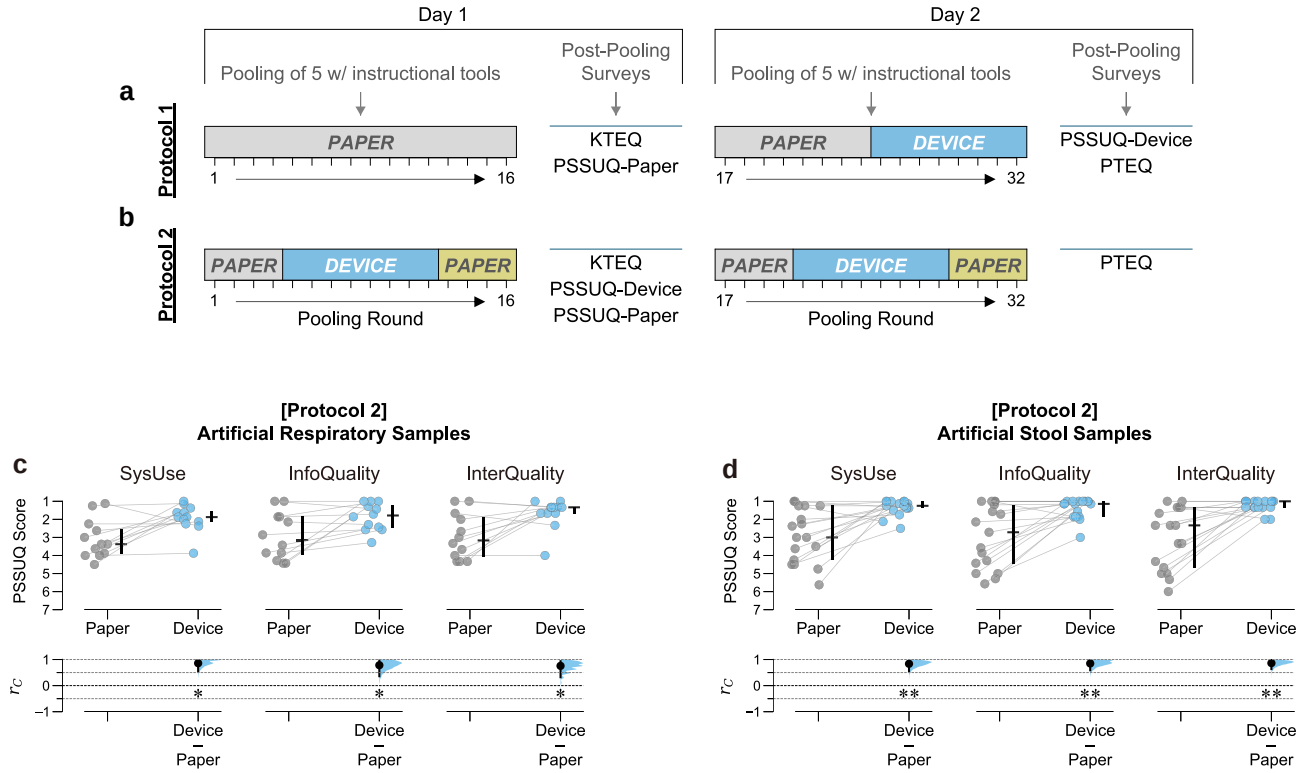

Figure 3 User study overview and self-reported results on usability surveys for instructional tools. a, b) Diagrams of pooling training workflows for protocol 1 (a) and protocol 2 (b) and subsequent surveys (KTEQ, Kirkpatrick training evaluation questionnaire; PSSUQ-Paper, poststudy system usability questionnaire for paper instructions; PSSUQ-Device, poststudy system usability questionnaire for instructional pooling device; PTEQ, posttraining effectiveness questionnaire). PAPER, paper-assisted pooling; DEVICE, device-assisted pooling. c, d) PSSUQ scores for system usefulness, information quality, and interface quality of day 1 paper instructions and instructional pooling device in protocol 2 groups using artificial respiratory (c) and artificial stool samples (d). The score follows a 7-point Likert scale; lower scores indicate better usability. In the upper graphs, horizontal and vertical bold lines represent the median and quantile ranges (Q1–Q3), respectively. Individual data points represent individual participants. In the lower graphs, effect sizes r_C (the matched-pairs rank biserial correlation coefficients (46)) were calculated using one-sided Wilcoxon signed-rank tests comparing PSSUQ scores between the paper instructions and the device. The effect sizes were displayed as filled dots with 95% CIs (vertical lines) and resampled distributions of effect sizes (curves) given the observed data. The magnitude of the effect using r_C is described by its distance from zero. $|r_C|$ (46, 47): 0.1 = small; 0.2 = medium; 0.3 = large; ≥0.4 = very large effect. Statistical significance was extracted from the one-sided Wilcoxon signed-rank tests with Benjamini–Hochberg correction (5% false discovery rate). Asterisks indicate significance levels: *P < 0.05; **P < 0.01. SysUse, system usefulness; InfoQual, information quality; InterQual, interface quality.

User performance was poor with paper instructions but improved significantly with the device. In protocol 1, participants showed poor performance (average $\text{err}_{\text{all}} \geq 1$, average $\text{Acc}_{\text{pool}} < 80\%$) during paper-assisted pooling on both day 1 and day 2 (Fig. 4a–d). Repetitive pooling with paper instructions did not result in improved performance ($r_C \sim 0$ and Hedges' $g \sim 0$) over all 24 rounds in either sample type (Fig. 4e–h and Tables S11 and S12), even in the analyses controlling for completion time spent on the pooling process (Fig. S10, Text S5, and Tables S13–S17). These objective measures contradict the subjective survey (KTEQ) results wherein participants reported skill acquisition from pooling with paper instructions on day 1.

Compared with the paper instructions, protocol 1 users exhibited improved performance when using the device. During the device-assisted pooling, all participants had significantly ($r_C \sim 1$) lower numbers of all uncorrected errors ($\sum \text{err}_{\text{all}}$) and significantly better (Hedges' $g \geq 1.5$) average volume-transfer accuracy (Avg. Acc_{pool}; Fig. 4e–h and Tables S11 and S12).

To identify what kinds of errors were prevalent, we classified errors into four categories: decontamination, sample transfer, contamination prevention, and documentation (Table S18), as either minor or severe. In the paper-assisted pooling, the most frequent errors observed (in ∼60% of users in each round) fell within the de-contamination category (Fig. 4i and j), most of which were classified as minor (Fig. S11a and Table S18). The second most frequent errors occurred in the documentation category, all of which were considered severe (Fig. S11a and Table S18). When using the device, nearly all users (respiratory: 10/10; stool: 9/10) avoided or corrected these minor and severe errors (Figs. 4i, j and S12a–d, Tables S19 and S20).

Protocol 2: device-enabled training for high-performance volume-transfer skills that persist after device removal

The quantitative performance metrics (i.e. err_{all}, $\text{err}_{\text{minor}}$, $\text{err}_{\text{severe}}$, and Acc_{pool}) were also analyzed for protocol 2 participants. The repeat crossover design of protocol 2 clearly demonstrates significantly improved performance (fewer human errors and higher volume-transfer accuracy) during device-assisted pooling, compared with paper-assisted pooling ($r_C \sim 1$; Hedges' $g > 0.9$) for both sample types (Fig. 5a–h and Tables S21 and S22).

The reduction in handling errors was observed only during device-assisted pooling. Except for severe errors from protocol

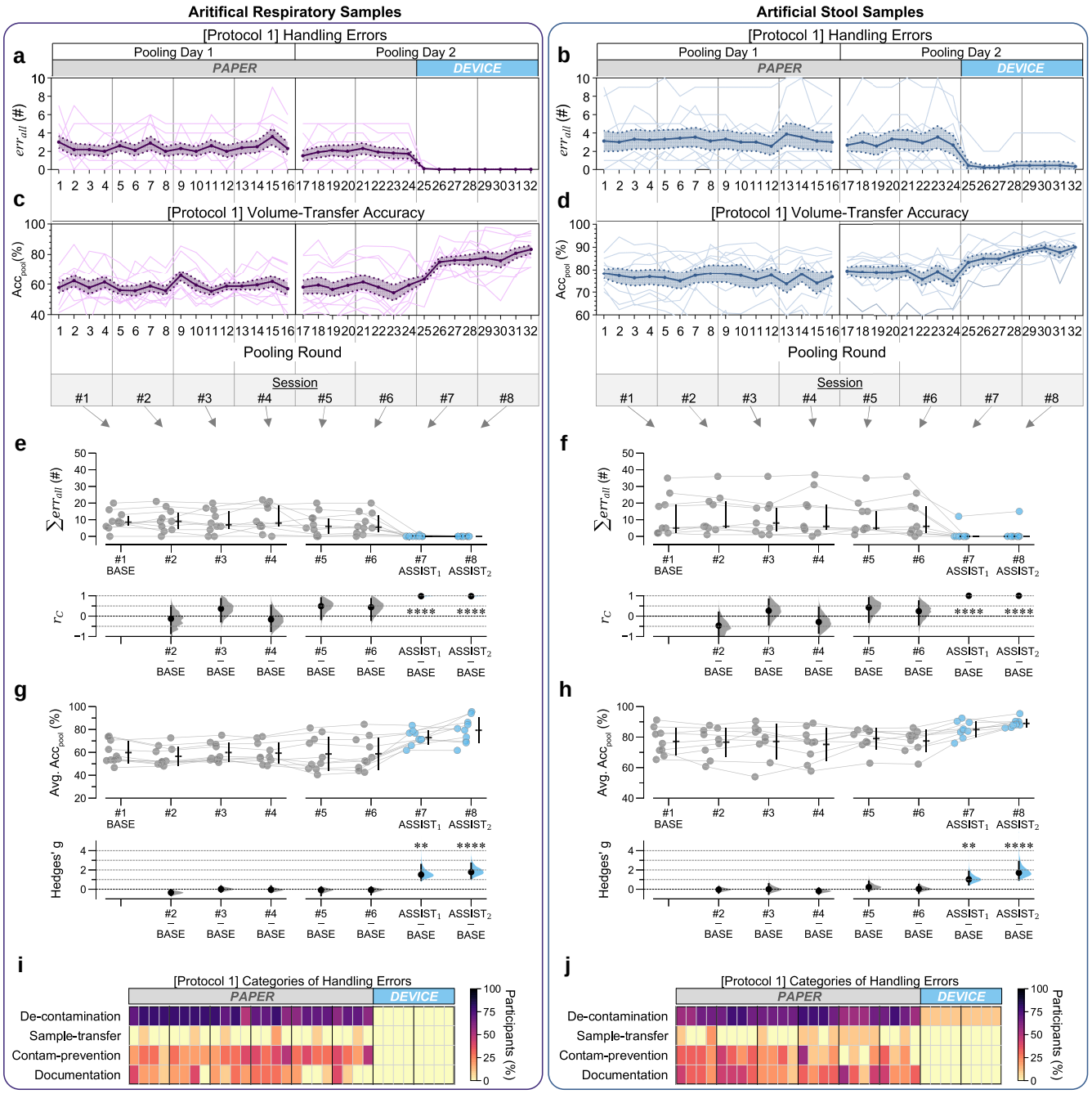

Figure 4 Assistive effects of instructional pooling device on user handling performance (errors and volume-transfer accuracy) in the protocol 1 group. a–d) Time course of all uncorrected handling errors (a, b) and volume-transfer accuracy (c, d) for artificial respiratory (a, c) and stool (b, d) samples across pooling rounds for protocol 1 group. Acc_{pool}, volume-transfer accuracy; err_{all}, all uncorrected handling errors. Semitransparent lines: individual participants; bold lines: the means of err_{all} (a, b) and Acc_{pool} (c, d) across participants; shaded area borders: ±1 SEM. e–h) Gardner–Altman estimation plots comparing the sum of err_{all} (e, f) and average Acc_{pool} (g, h) across pooling sessions (1 session = 4 pooling rounds). In the upper graphs, horizontal bold lines represent the median for non-normal data (e, f) and the mean for normal data (g, h). Vertical lines represent quartile ranges (e, f) or ±1 SEM (g, h). Data points represent participants. Σerr_{all}, sum of err_{all}; Avg. Acc_{pool}, average Acc_{pool}. In the lower graphs, effect sizes r_C (e, f) and Hedges' g (g, h) are shown from the comparison of the performance between the first session (#1, BASE) and each of the other sessions (#2–#8). r_C (e, f) and Hedges' g (g, h) were calculated using one-sided Wilcoxon signed-rank tests and one-sided, paired Student's t tests, respectively. The magnitude of the effect using r_C and Hedges' g is described by its distance from zero. $|r_C|$ (46, 47): 0.1 = small; 0.2 = medium; 0.3 = large; ≥0.4 = very large effect. Hedges' g (46): 0.2 = small; 0.5 = medium; 0.8 = large effect. Effect sizes are displayed as filled dots with 95% CI (vertical lines) and resampled distributions (curves). Statistical significance levels: *$P < 0.05$; **$P < 0.01$; ***$P < 0.001$; ****$P < 0.0001$ (extracted from the fixed effects of linear mixed-effect models using dummy coding). i, j) Heat maps showing the proportion of protocol 1 participants making errors in four categories across 32 pooling rounds over two nonconsecutive days. Color intensity indicates the percentage of participants making errors in each category per round.

2/stool group, error counts ($\sum err_{minor}$, $\sum err_{severe}$, and $\sum err_{all}$) increased when participants used paper instructions, even after using the device ($|r_C| < 0.5$; BASE vs. $AFTER_2$; Figs. 5e, f and S12e–h, Tables S21, S23, and S24). Error patterns remained consistent for individual participants before and after the device use (Figs. 5i, j, S11b, and S13). These results indicate that device-assisted pooling in protocol 2 was insufficient to train users to avoid handling errors when not using the device.

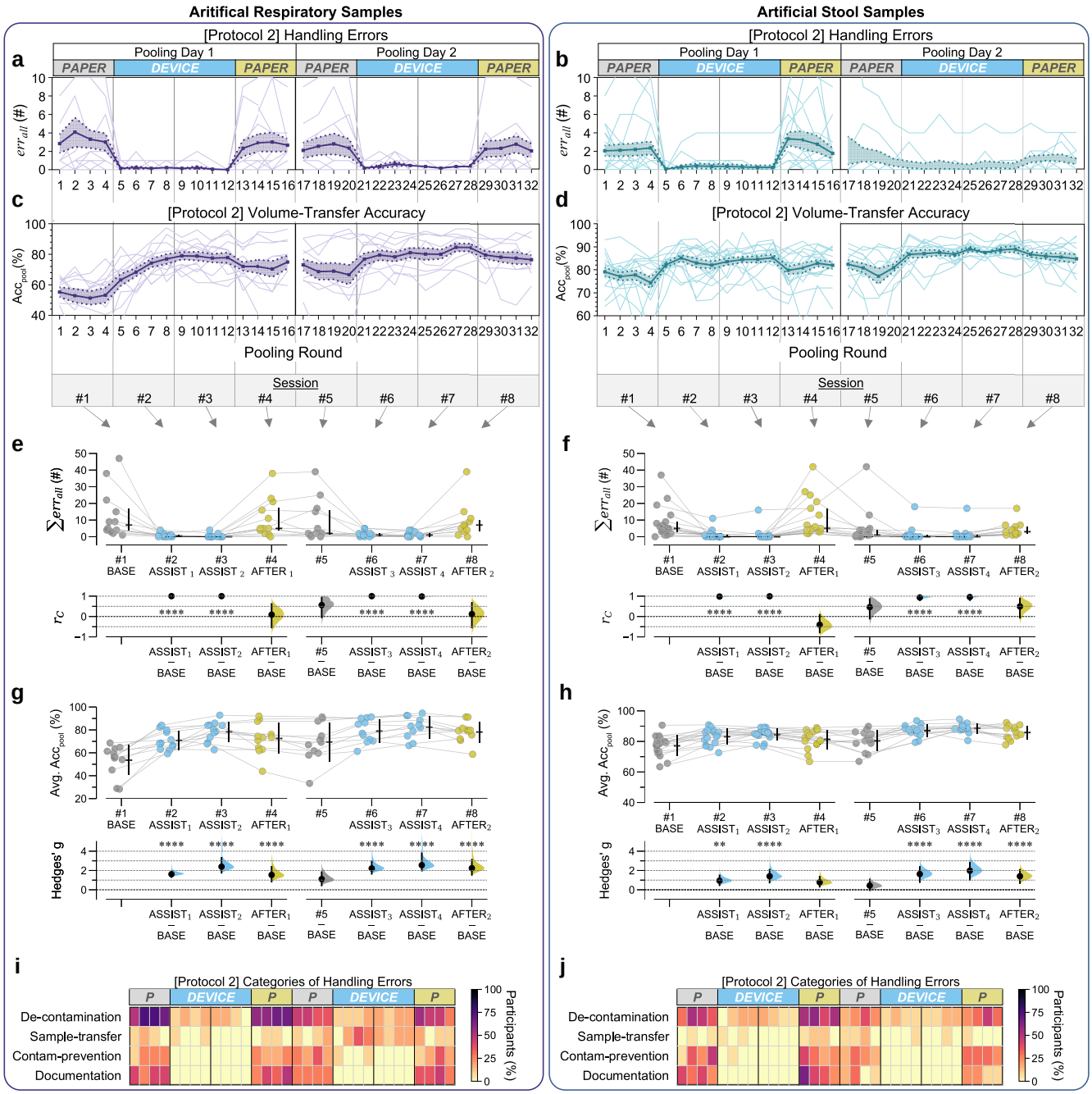

Figure 5 Assistive and training effects of instructional pooling device on user performance (errors and volume-transfer accuracy) in the protocol 2 group. a–d) Time course of all uncorrected handling errors (a, b) and volume-transfer accuracy (c, d) for artificial respiratory (a, c) and stool (b, d) samples across pooling rounds for protocol 2 group. Semitransparent lines: individual participants; bold lines: the means of handling errors (a, b) and accuracy (c, d) across participants; Shaded area borders: ±1 SEM. e–h) Gardner–Altman estimation plots comparing the sum of all uncorrected errors (e, f) and average volume-transfer accuracy (g, h) across pooling sessions. In the upper graphs, horizontal bold lines represent the median for non-normal data (e, f) and the mean for normal data (g, h). Vertical lines represent quartile ranges (e, f) or ±1 SEM (g, h). Data points represent participants. In the lower graphs, effect sizes r_C (e, f) and Hedges' g (g, h) are shown from the comparison of the performance between the first session (#1, BASE) and each of the other sessions (#2–#8). r_C (e, f) and Hedges' g (g, h) were calculated using one-sided Wilcoxon signed-rank tests and one-sided, paired Student's t tests, respectively. The magnitude of the effect using r_C and Hedges' g is described by its distance from zero. $|r_C|$ (46, 47): 0.1 = small; 0.2 = medium; 0.3 = large; ≥0.4 = very large effect. Hedges' g (46): 0.2 = small; 0.5 = medium; 0.8 = large effect. Effect sizes are displayed as black dots with 95% CI (vertical lines) and resampled distributions (curves) given the observed data. Statistical significance levels: *$P < 0.05$; **$P < 0.01$; ***$P < 0.001$; ****$P < 0.0001$ (extracted from results of linear mixed-effect models using dummy coding). i, j) Heat maps showing the proportion of protocol 2 participants making handling errors in four categories across 32 pooling rounds over two nonconsecutive days. Color intensity indicates the percentage of participants making errors in each category per round.

In contrast, the device produced a training effect on volume-transfer accuracy, even after the participants were no longer using the device. Individual participants showed improved volume-transfer accuracy (Avg. Acc_{pool}; Hedges' $g > 1$) during device-assisted pooling ($ASSIST_{1–4}$) and maintained high accuracy (Hedges' $g > 0.5$) in the postdevice session ($AFTER_{1,2}$; Fig. 5g, h and Table S19).

Although participants performed slowly with the device (Fig. S10), these assistive and training effects of the device on error

metrics and Acc_{pool} in protocol 2 remained statistically significant even in the analyses controlling for completion time as a covariate (Text S5 and Tables S25–S29). There was no statistically significant difference in the baseline performance (for all metrics; err_{all}, err_{minor}, err_{severe}, and Acc_{pool}) between protocol 1 and protocol 2 groups ($P > 0.05$; interaction terms comparing session #1 in the linear mixed-effect analyses). Both accuracy and handling errors were also independent of the interval between day 1 and day 2 (Fig. S14), which differed among participants (median [Q1, Q3]: 7 [4, 8] days).

Use of the device resulted in high-performance volume transfer, which was determined by the number of high-quality pools showing high accuracy ($Acc_{pool} \geq 80\%$) and precision ($CV_{pool} \leq 25\%$) per pooling round (Text S6 and Fig. S15). Participants produced high-quality pools in both device-assisted ($ASSIST_{1-4}$) and postdevice sessions ($AFTER_{1-2}$) significantly more ($r_C < -0.5$) than those in the first paper-assisted session (BASE; Fig. S16a–d and Tables S30 and S31). In protocol 2, 15 participants (72.4% in respiratory; 53.8% in stool) showed significant performance improvements (adjusted $P < 0.05$; BASE vs. $ASSIST_4$), with 14 of these participants maintained their high performance in the postdevice session ($AFTER_2$; Fig. S16e, f and Table S32). These results suggest both assistive and training effects for volume-transfer skills.

The device enables users to achieve high-performance pooling of artificial clinical samples

We next investigated whether the device could enable users to achieve high-performance pooling, defined as high-accuracy and high-precision volume transfer ($Acc_{pool} \geq 80\%$ and $CV_{pool} \leq 25\%$) and perfect handling ($err_{all} = 0$).

Considering all quantitative metrics, the device significantly ($r_C \sim -1$) assisted users in achieving high-performance pooling for both sample types (Fig. 6a–d and Figs. S17–S19 and Tables S33 and S34). The assistive effects were significant (adjusted $P < 0.05$) for most individuals (58.3–72.7% in the respiratory group; 76.5–76.9% in the stool group) shown in device-assisted sessions #3 and #7 (Fig. 6e, f and Table S35). Consequently, up to 92.8% of participants achieved high-performance pooling in ≥2 of 4 pooling rounds during the last device-assisted session #7 ($ASSIST_4$).

The device helps users create trackable pools with five consistent sample volumes and avoid poor-quality pools

Despite the significant assistive/training effects, a critical question remained: would these improvements translate to pools suitable for trackable and reliable pooled molecular testing? To address this question, we categorized pools into three classifications, defined in Table S36: "Correct," "Incorrect," and "Invalid" with additional subclassifications for types. Correct pools are generated when participants accurately follow instructions and properly transfer individual samples. Incorrect pools result from procedural user errors that are not corrected nor avoided. Invalid pools result from the poor pool quality. They include those with a maximum mass pooling ratio (MPR_{max}) ≥ 10, where MPR_{max} is defined as the ratio of the pool's final weight to the minimum weight among any individual sample within the pool. A common cause of Invalid pools is inconsistent sample volumes, which could cause false diagnostic negative results, particularly when an insufficient volume of a weak-positive sample is pooled with negative samples.

Device-assisted pooling significantly reduced Incorrect pools and increased the proportion of Correct pools compared with paper-assisted pooling (Fig. 7a–d). When using the device, protocol 2 users produced zero Incorrect pools (out of 424 pools), whereas with paper-assisted pooling they produced 135 Incorrect pools (31.8%) out of 424 total pools (Fisher's exact test, $P < 0.0001$; Table S37).

Crucially, the device was able to identify Invalid pools of the three types (Table S36). Through weight measurement, the device tracked individual pooled sample weights, total pooled sample weights, and volume-transfer activities during pooling. In parallel, the real-time monitoring of all tubes and caps verified that the sample was correctly transferred from an opened individual tube into the pooling tube. As a result, a total of 22 Invalid pools were identified: 18 Invalid type (1) pools with large MPR_{max} (10–100) from eight participants; one combined Invalid type (1) and type (2) pool (total volume: 516 μL; MPR_{max}: 24.3) from one participant; and three Invalid type (3) pools from participants who accidentally removed samples from pooling tubes (Fig. 7e–g). In contrast, nearly three times as many (64) Invalid pools were generated during the paper-assisted pooling (Figs. 7a–d, S20, and S21); as paper-assisted pooling does not have built-in verification of sample transfer, these Invalid pools would likely go unrecognized in a clinical laboratory setting without the device.

The device supports reliable pooling of clinical STH samples to enable high-performance pooled NAAT

To demonstrate the utility of the device for the pooling of clinical samples prior to NAAT, we used the device to create five-sample pools using 42 archived clinical stool specimens from the previous field study of STH infections in children in Bangladesh (see Materials and methods) (48). Among these 42 archived specimens, 21 had previously tested positive for the STH *Ascaris lumbricoides* DNA (Fig. 8a). Each individual sample was randomly selected, and a biosafety-trained researcher used the instructional pooling device to pool each clinical sample with four (control) stool samples from healthy human donors.

The device demonstrated high-precision pooling (average CV <5% in volume transfer) of homogenized human stool suspensions (Fig. 8d). The MPR of each clinical sample within a pool was close to the ideal value of 5 (mean: 4.998; SD: 0.2459; Fig. 8b and c). No significant differences were observed between the pooled weight of individual STH clinical and control stool suspensions (Kruskal–Wallis test, $P = 0.314$; Fig. 8e and Table S38). For *A. lumbricoides* detection by NAAT (qPCR), the device-assisted pooling showed a mean cycle quantification shift (ΔCq; $Cq_{Pool} - Cq_{Indiv}$) of 2.19 (95% CI = [2.06, 2.31]); this Cq shift is close to the expected shift ($\log_2 5 \sim 2.32$) for pools of 5, leading to a strong linear relationship between Cq_{indiv} and Cq_{pool} for

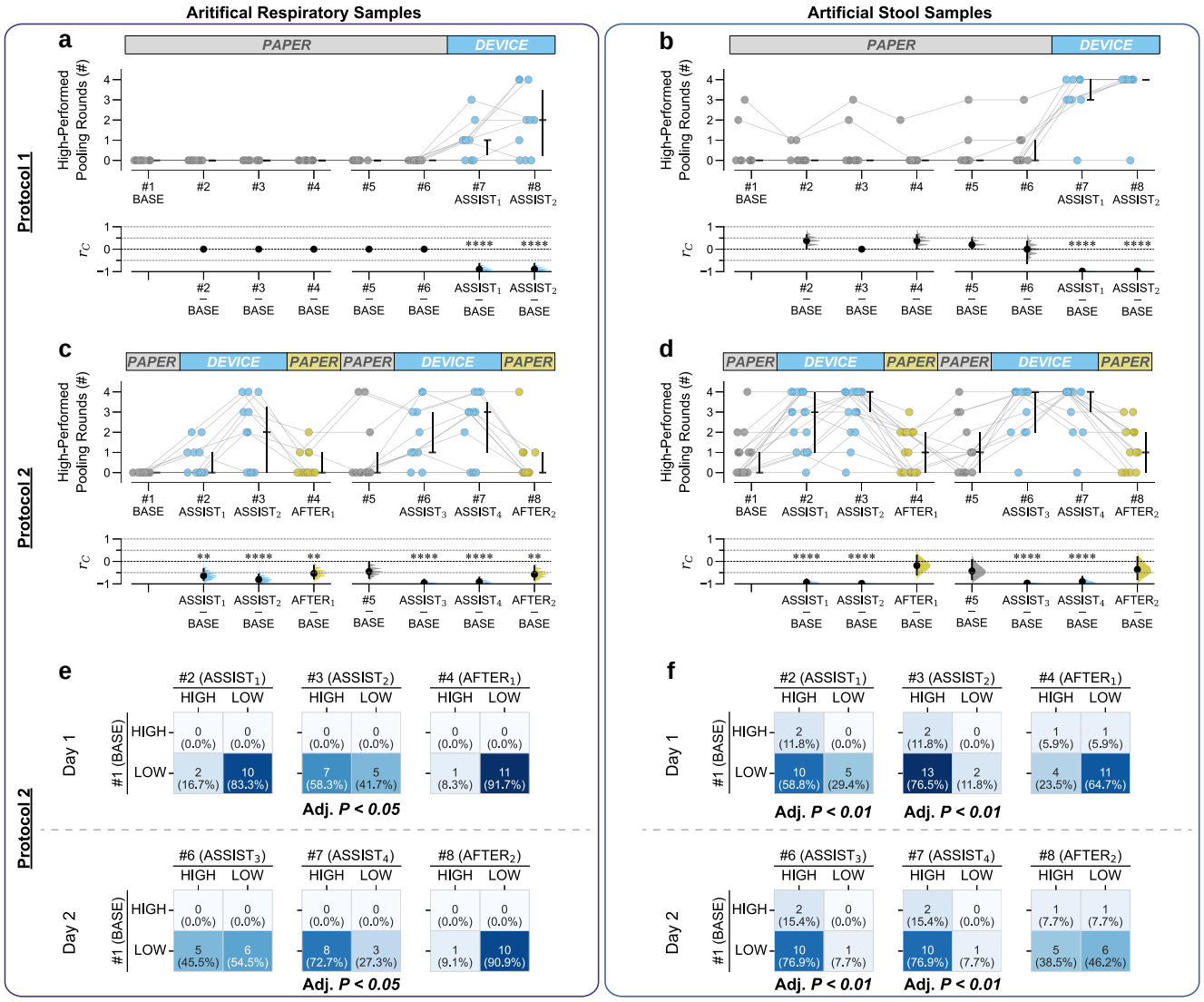

Figure 6 Device-assisted high-performance sample pooling, defined as pooling with volume-transfer accuracy $Acc_{pool} \geq 80\%$, precision $\leq 25\%$ CV_{pool}, and perfect handling (i.e. $err_{all} = 0$). a–d) Gardner–Altman estimation plots comparing the number of high-performance pooling rounds between the first pooling session (#1, BASE) and subsequent sessions (#2–#8) in protocol 1 (a, b) and protocol 2 groups (c, d). Upper graphs: data points with the median (horizontal bold lines) and quartile ranges (vertical lines) for individual participants. Lower graphs: Effect sizes r_C (filled dots) from one-sided Wilcoxon signed-rank tests with 95% CI (vertical lines) and resampled distributions (curves). The magnitude of the effect using r_C is described by its distance from zero. $|r_C|$ (46, 47): 0.1 = small; 0.2 = medium; 0.3 = large; ≥0.4 = very large effect. Statistical significance levels: $^*P < 0.05$; $^{**}P < 0.01$; $^{***}P < 0.001$; $^{****}P < 0.0001$ (extracted from results of linear mixed-effect models using dummy coding). e, f) 2 × 2 contingency tables for McNemar's tests comparing sample-pooling performance of protocol 2 participants between the first pooling session #1 (BASE) and one of sessions #2–#8 separated by high ("HIGH") and low ("LOW") performers. Color value (light to dark) highlights the relative distribution of participants within each individual 2 × 2 table, with darker colors indicating cells containing higher percentages. Note that the color-value scale is applied across all contingency tables within each sample type. Cell values: number of participants in each performance category combination. HIGH, high performers who achieved ≥2 rounds of high-performance pooling during a 4-round session. LOW, low performers who achieved <2 rounds of high-performance pooling during a 4-round session. *P* values for statistical significance were determined by McNemar's tests with Benjamini–Hochberg correction (5% false discovery rate).

STH-positive specimens (Fig. 8f). Perfect agreement was observed between STH diagnostic results from individual testing and five-sample pools generated using the device (Fig. 8g).

Discussion

The rapid advancement of AI and automation technologies is reshaping global labor markets, creating an urgent need to develop effective strategies for workforce adaptation. Simultaneously, the persistent inaccessibility of high-performance molecular diagnostic testing remains one of the greatest barriers to global infectious-disease eradication efforts, particularly in RLS. Diagnostic shortages for major diseases (e.g. bloodborne, respiratory, and STH), and testing backlogs during surges (e.g. COVID-19 pandemic) stem from the high cost per test, error-prone workflows, and a lack of trained laboratory personnel.

This work (Fig. 1) addresses all of these challenges by both assisting and training laboratory-naive personnel to perform the complex workflow of sample pooling, which has the potential to reduce the per-test diagnostic cost (without sacrificing test performance) and improve the workforce in RLS. The device

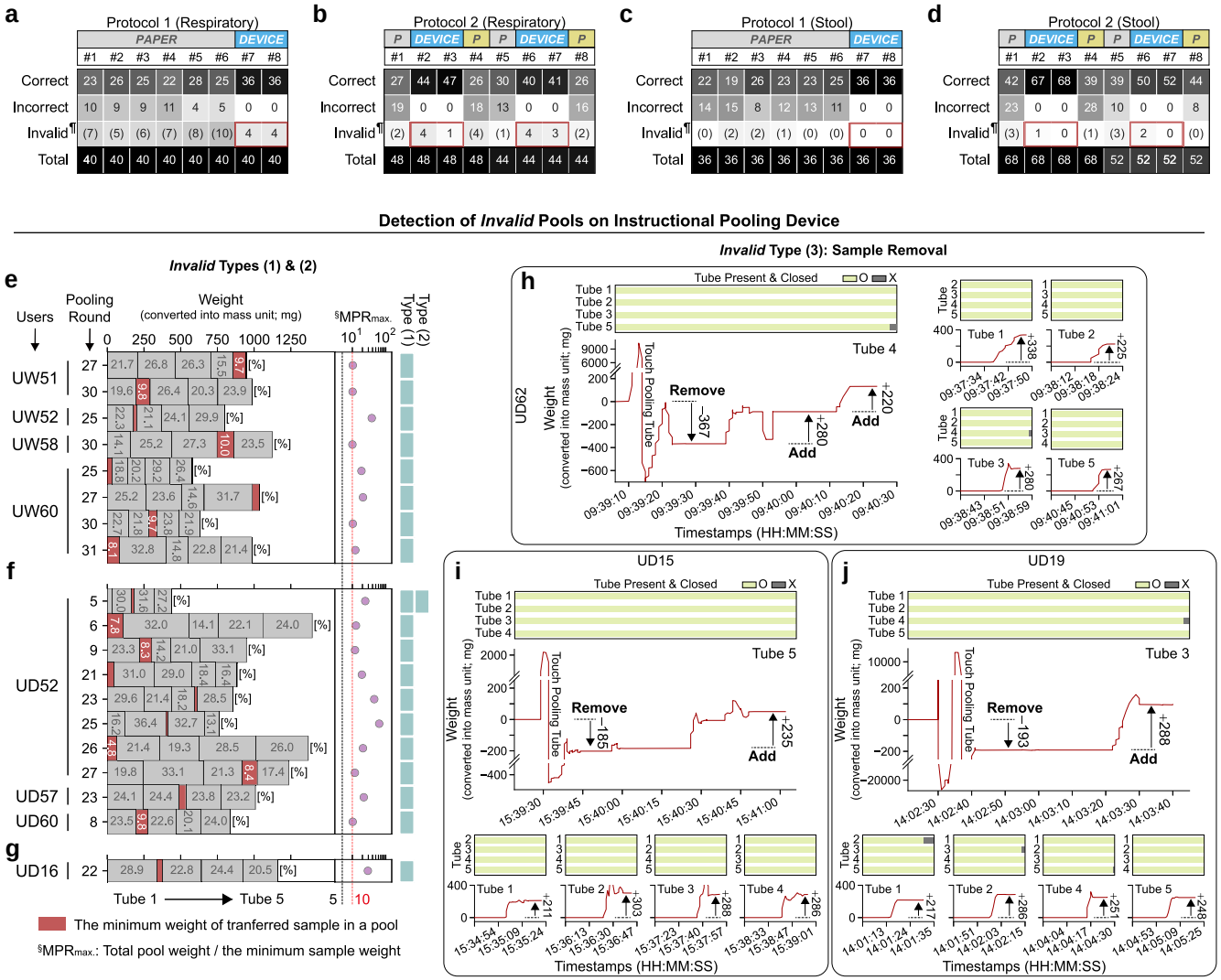

Figure 7 "Correct," "Incorrect," and "Invalid" pools (as defined in Table S36) produced during the user study. a–d) Number of pools produced across pooling sessions #1–#8 in protocol 1 (a, c) and protocol 2 (b, d) groups using artificial respiratory (a, b) and stool samples (c, d). Correct, Incorrect, and Invalid pools are defined in Table S36. ¶Pools that fall into both Incorrect and Invalid categories are counted as Incorrect. e–g) Device-detected Invalid types (1) and (2) pools produced by protocol 1 (e) and protocol 2 (f, g) groups using artificial respiratory (e, f) and stool samples (g). Each horizontal bar represents a pool of five samples (tubes 1–5), with weight percentages. MPR_{max}, defined as the ratio of total pool weight to the minimum sample weight, is shown for each Invalid pool. The lowest weight sample from each pool is highlighted (numbers in white in red boxes). Invalid subtype classifications are indicated by the adjacent vertical markers in the Type (1) and Type (2) columns. h–j) Device-detected Invalid type (3) pools through real-time monitoring of volume-transfer activities by users UD62 (h), UD15 (i), and UD19 (j) during rounds 23rd, 5th, and 24th, respectively. The weight–time plots in each panel show measured weight changes in the pooling tube during the volume transfer in a single round. The large plot shows inappropriate activities where a sample was removed from the pooling tube (remove) before adding a sample (add) from an opened tube: tubes 4 (h), 5 (i), or 3 (j). Small inlet plots show proper activities where samples were correctly transferred from other tubes to the pooling tube. Horizontal bars indicate real-time monitoring of tube presence and cap status in the device (lighter color value bars marked O: tube present and capped; darker color value bars marked X: tube absent or uncapped) for all other tubes. Numbers adjacent to arrows indicate the weight (mg) of transferred sample.

(Fig. 2) is designed for a low-cost, open-source platform (~$600 USD; Table S39), with further cost reductions possible through mass production and local sourcing. It features a user-friendly design for seamless workflows, real-time error monitoring, pool-quality control, and documentation capabilities. To support pooled testing across a range of disease prevalence scenarios, future work will extend the platform to flexible pooling strategies. Owing to its modular architecture, incorporating additional barcode-embedded tube modules (estimated cost per module: ~$60.6) could increase tube-processing capacity, thereby enabling larger pooling sizes (e.g. 6–10 samples or more). Similarly, different transfer volumes (e.g.10–1,000 µL) can be supported using commercially available disposable transfer pipettes in combination with the scale module that can accurately measure in that range (Fig. S5).

The user study (Figs. 3–7) demonstrated the utility of the device for assisting and training laboratory-inexperienced personnel to perform sample pooling. Compared with paper instructions, device use reduced uncorrected handling errors ($|r_C| \sim 1$) and raised mean volume-transfer accuracy (Hedges' $g > 1$). Device users retained better volume-transfer skills even after device removal, supporting training features of the device beyond its procedural assistance. Analyses controlling for completion time suggest that performance gain and skill acquisition

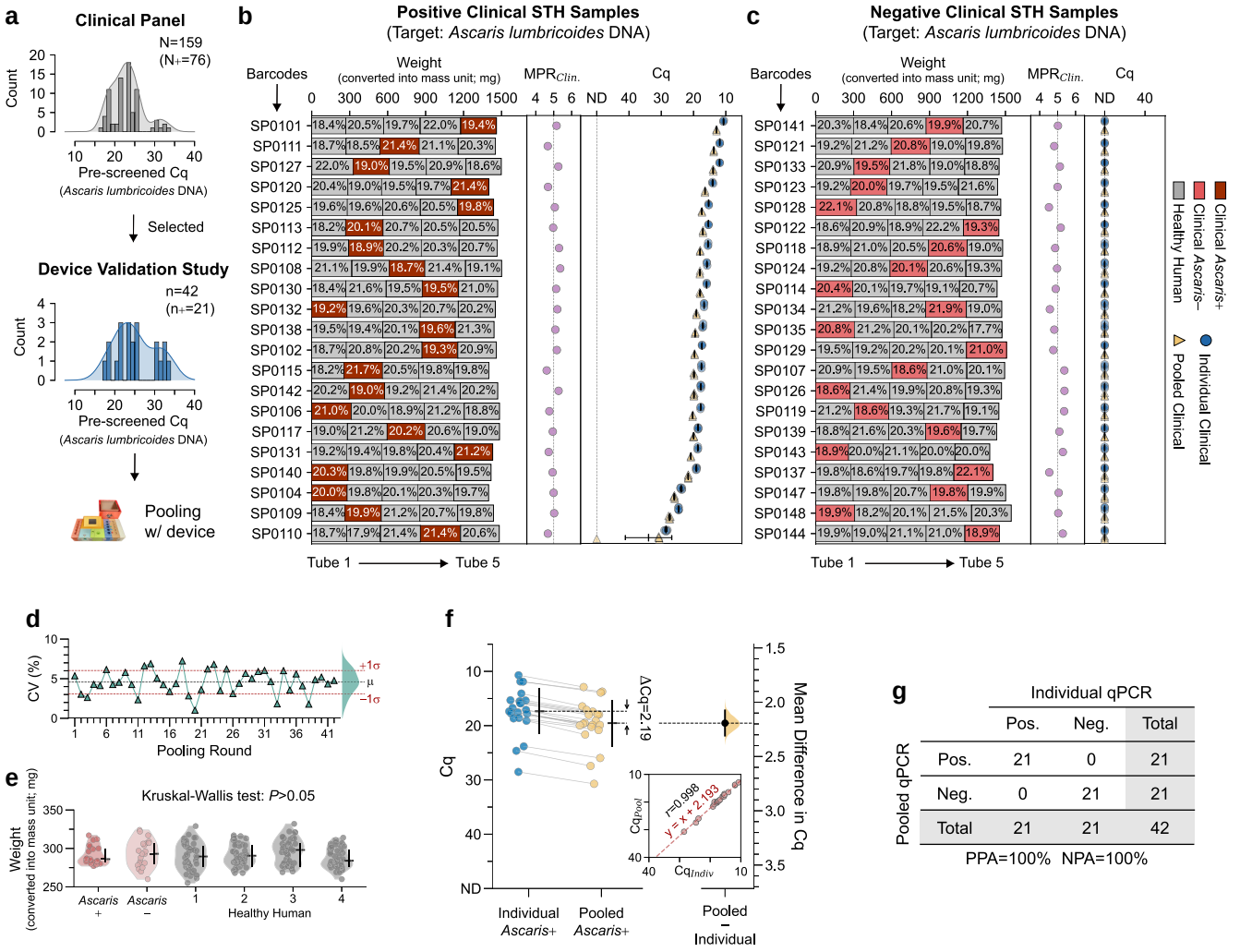

Pooled qPCR	Individual qPCR: Pos.	Neg.	Total
Pos.	21	0	21
Neg.	0	21	21
Total	21	21	42

Figure 8 Device-validation study for clinical sample pooling to detect *A. lumbricoides* DNA from human stools collected from children in STH-prevalent regions. a) Distribution of prescreened Cq values of *A. lumbricoides* DNA from archived clinical samples (n = 159; 76 positives, 83 negatives). For this study, 42 samples (21 positives, 21 negatives) were selected through stratified random sampling to obtain a range of Cq values. b, c) Weight distribution of five individual stool suspensions (one clinical and four healthy human) per pool. Barcodes represent unique identifiers for individual clinical samples, arranged by ascending Cq values. Horizontal bars represent a pool of five individual samples (tubes 1–5), with the weight percentages. The highlighted segment in each horizontal bar indicates the clinical stool suspension, either clinical positive (b) or negative (c) for *Ascaris lumbricoides* DNA. The remaining segments indicate commercial stool suspensions from healthy human donors. The sequential position of the clinical STH sample was randomized among the four commercial samples in each pooling round. $MPR_{Clin.}$: mass pooling ratio in respect to each clinical sample (total pool weight/individual clinical sample weight). Cq values of all qPCR replicates in this study are shown for individual clinical and pooled samples. Vertical lines: mean; horizontal lines: SD. d) CV values across pooling rounds. The density curve shows the CV distribution. The central solid line indicates the mean (μ = 4.56%) and the flanking dashed lines indicate ±1 SD (σ = 1.47%). e) Weight distributions of suspensions transferred from 21 clinical positives (Ascaris+), 21 clinical negatives (Ascaris−), and four unique healthy human samples to pools. Horizontal lines: median; vertical lines: quantile ranges (Q1–Q3). f) Estimation plot comparing paired Cq values between individual (Cq_{Indiv}) and pooled positive samples (Cq_{Pool}). Horizontal lines: mean; vertical lines: SDs. The mean Cq difference (ΔCq = 2.19) shown with 95% CI (vertical line) and resampled distributions of difference (curves). Inlet: correlation plot (Pearson's r: 0.998). g) 2 × 2 contingency table showing positive percent agreement (PPA) and negative percent agreement (NPA) of pooled versus individual qPCR testing.

were primarily driven by the device, rather than slower pacing alone (Text S5). Notably, the Dunning–Kruger effect was evident among protocol 1 participants, who reported strong perceived skill gains despite no significant improvements in objective performance during the paper-assisted pooling on day 1. This discordance highlights the importance of objective analytics and real-time quantitative feedback to foster true skill acquisition and prevent false confidence (49) that can cause diagnostic errors (50). Finally, unlike low-cost liquid handlers, the device recorded the actual weight of each pooled sample during pooling, enabling detection of Invalid pools that could otherwise lead to diagnostic errors.

The device-validation study (Fig. 8) using 42 remnant clinical STH samples demonstrated the utility of the device for clinical sample pooling in disease surveillance or screening in RLS. Device-assisted five-sample pooling yielded 100% positive/negative agreement for pooled qPCR in this sample set, suggesting the potential to transform STH-surveillance economics (34) by driving down per-sample analysis costs while yielding diagnostic performance superior to the gold-standard Kato–Katz technique (16). Current STH analyses are performed by manual DNA extraction followed by qPCR assays (16, 34, 48); therefore, pooling of raw samples upstream of DNA extraction would reduce the cost of analysis (e.g. from $11 to <$3) and increase the throughput of analysis (34). By

facilitating easier adoption of pooling in RLS, device-assisted high-performance surveillance would facilitate timely decisions on whether to cease MDA where STH prevalence is sufficiently low.

Beyond STH, the same instructional pooling paradigm could be adapted for universal screening: by pairing with POC molecular diagnostics (e.g. Cepheid GeneXpert (31–33)), the device provides a pathway to increase testing throughput for bloodborne pathogens (e.g. HIV (28, 29) and HCV (30, 31)), respiratory diseases (e.g. TB (32) and viral infections (33)), and other infections in RLS. The device could also be invaluable during testing surges, so that even minimally trained personnel could be enlisted to help meet increased testing demands. This work exemplifies how new technologies, with affordability and usability, can extend healthcare capacity while employing newly trained workers for healthcare services, rather than replacing them (51–53).

This work highlights the potential of this class of devices for use in RLS, where automated instruments are often impractical for preanalytical sample processing—tasks that humans can perform more efficiently with appropriate guidance (54). Diagnostic workflows involving clinical specimens, such as stool homogenization (STH) (34), blood/plasma separation (HIV/HCV) (55), and sputum evaluation (TB) (56), frequently involve complex manual steps, precise volume-transfer skills, and visual judgment. These activities are challenging for low-cost automated systems due to pipetting failures, clogging, and inability to perform visual judgments (57–59). By assisting and training laboratory-inexperienced personnel to successfully perform complex tasks (e.g. pooling), this class of devices can facilitate task-shifting in settings where individuals often perform multiple roles. This integration of technology with human capabilities supports more sustainable and scalable delivery of diagnostic services at the point of need.

We acknowledge several limitations of this work. First, this study does not directly measure cross contamination, and future work will include experimental validation. Second, the user-study cohort of 48 participants was skewed toward young adults. Training protocols spanned two nonconsecutive days, so longer-term skill retention remains to be studied. Artificial samples were prepared to approximate, but may not have fully replicated, the physical properties of actual clinical specimens. Printed instructions were chosen as the control because paper-based instructions remain the primary training resource in many resource-limited laboratories; however, richer comparators (e.g. a one-time instructional video) could better mirror real-world onboarding and should be evaluated in future work. Furthermore, the device-validation studies with STH were performed by an engineer who underwent proper biosafety training, as untrained personnel were not allowed to handle biohazardous materials (e.g. clinical samples) under Caltech biosafety policies. These precautions were intended to ensure safe handling of clinical STH stool samples that may contain infectious agents, including STH pathogens and poliovirus. Future work will extend the device's instructional capabilities to include a basic biosafety-training session, followed by multilocation field trials under representative conditions.

This class of train and assist biomedical devices sits at the intersection of two domains: labor and human health. Beyond pooling, broader development and adoption of devices in this class could help mitigate both the labor crisis and healthcare inequities. Importantly, as new technologies disrupt labor markets, there remains a critical time window to implement scalable, pragmatic retraining solutions before inequalities widen further. We hope that this publication, the publicly available data, and open-source designs accompanying this work will stimulate development of innovative devices in this class to strengthen workforce and expand healthcare access.

Materials and methods

In the SI Appendix, Methods, we provide a comprehensive list of materials for the fabrication of the eight-module instructional pooling device and its disposable trays, detailing polymer filaments, sensor packages, microelectronics, and vacuum forming. We then discuss descriptions of device fabrication for each module and its polypropylene device-protective trays, as well as the dual-microcontroller architecture that coordinates display, barcode scanning, object detection, precision weighing, and Bluetooth data export. We then outline the methods for expected handling movement and the calibration of the strain-gauge microbalance of the device. We present the design of the user study with underlying hypotheses and the details for participant recruitment, eligibility, withdrawal, compensation, and demographic statistics. We describe the details for preparing the user study: the preparation of a customized data logger, sample-collection tubes, and artificial samples. Experimental settings, data collection methods, and detailed procedures for pooling exercises in the user study are also described. Details for data analysis of the user study data are described—paired statistical tests, linear mixed-effects modeling, and effect-size estimation, which were used to analyze the assistive and training effects on accuracy, precision, error counts, and task duration. Finally, we describe the methods for the device-validation study that was conducted for a five-sample pooling validation of clinical STH stool samples on the device, detailing clinical sample preparation, pooling procedure, DNA extraction, qPCR conditions, and positive/negative percent agreement calculations. Full details for Materials and methods are described in Methods S1—S22. Inclusion and ethics statements are available in Text S8. The text of the manuscript was proofread and revised by using OpenAI GPT-4o and o3 models and the Claud Sonnet 3.7 model.

Acknowledgments

The authors thank A. E. Romano (Caltech), M. Cooper (Caltech), R. Lazarovits (Caltech), O. Pradhan (Caltech), N. J. Wu-Woods (Caltech), R. Akana (Caltech), M. K. Porter (Caltech), M. K. Kim (Caltech), S. Haynes (Smith College), and A. M. Gonzalez (Smith College) for helping this work. Images of lab-inexperienced personnel, specimen tubes, workers, and individual POC NAAT in Fig. 1 were created in BioRender. (2026) https://BioRender.com/j98r312. Detailed acknowledgement statements are available in Text S10.

Supplementary Material

Supplementary material is available at *PNAS Nexus* online.

Competing Interests

The work in this paper is the subject of a patent application filed by Caltech (R.F.I., M.L., and S.H.J.). The other authors declare no competing interests.

Funding

This work was funded in part by an Innovation Seed grant from the Merkin Institute for Translational Research (Caltech) and the Jacobs Institute for Molecular Engineering for Medicine (Caltech).

Author Contributions

Minkyo Lee (Conceptualization, Data curation, Formal analysis, Investigation, Methodology, Validation, Visualization, Writing—original draft), Xinyue (Penny) Pei (Formal analysis, Investigation, Methodology, Validation, Visualization, Writing—review & editing), Si Hyung Jin (Conceptualization, Investigation, Visualization, Writing—review & editing), Natasha Shelby (Data curation, Investigation, Visualization, Writing—review & editing), Rani Gera (Formal analysis, Validation, Writing—review & editing), Alexander Viloria Winnett (Formal analysis, Investigation, Methodology, Visualization, Writing—review & editing), Colin F. Camerer (Methodology, Writing—review & editing), Mahbubur Rahman (Investigation, Methodology, Resources, Writing—review & editing), Nils Pilotte (Methodology, Resources, Writing—review & editing), Steven A. Williams (Methodology, Resources, Writing—review & editing), and Rustem F. Ismagilov (Conceptualization, Funding acquisition, Project administration, Resources, Supervision, Writing—review & editing). Detailed author contribution statements are available in Text S9.

Data Availability

The datasets generated and analyzed during the current study, including all device designs and related codes, are available at CaltechDATA: https://doi.org/10.22002/qsx5j-53280. All statistical analysis results are available in Tables S1–S44.

References

1. World Economic Forum. *The future of jobs report 2025*. World Economic Forum, 2025.
2. Hazan E, *et al. A new future of work: the race to deploy AI and raise skills in Europe and beyond*. McKinsey Global Institute, 2024.
3. Cazzaniga M, *et al.* 2024. Gen-AI: Artificial Intelligence and the Future of Work. Staff Discussion Notes, 2024(001), 1–41. https://doi.org/10.5089/9798400262548.006
4. Autor DH. 2022. The Labor Market Impacts of Technological Change: From Unbridled Enthusiasm to Qualified Optimism to Vast Uncertainty. *NBER Working Paper No.* w30074 [Preprint]. https://ssrn.com/abstract=4122803 (accessed 2 June 2025).
5. Leber AL, Peterson H, Bard JD. 2022. The hidden crisis in the times of COVID-19: critical shortages of medical laboratory professionals in clinical microbiology. *J Clin Microb*. 60: e00241–e00222.
6. Ronny FMH, Sherpa T, Chosang T, Ahmad S. 2023. Looking into the laboratory staffing issues that affected ambulatory care clinical laboratory operations during the COVID-19 pandemic. *Lab Med*. 54:e114–e116.
7. Garcia E, Kundu I, Kelly M, Soles R. 2024. The American Society for Clinical Pathology 2022 Vacancy Survey of medical laboratories in the United States. *Am J Clin Pathol*. 161: 289–304.
8. Bureau of Labor Statistics, U.S. Department of Labor. "Clinical Laboratory Technologists and Technicians" in *Occupational Outlook Handbook*, (U.S. Department of Labor, 2025). https://www.bls.gov/ooh/healthcare/clinical-laboratory-technologists-and-technicians.htm. Accessed 2 June 2025.
9. Employment and Social Development Canada, Data from "Canadian Occupational Projection System (COPS)—2024 to 2033 projections." Canada.ca. https://open.canada.ca/data/en/dataset/e80851b8-de68-43bd-a85c-c72e1b3a3890/resource/da1135c5-a1df-4a07-a81e-de308ae6cce6. Deposited 12 February 2025.
10. National Foundation for Educational Research, Data from "Supply of skills for jobs in science and technology." GOV.UK. https://explore-education-statistics.service.gov.uk/data-catalogue/data-set/7c4f23df-1d18-4979-b8d2-1d48b53326f6. Deposited 9 May 2024.
11. Ashraf AA, Rai S, Alva S, Alva PD, Naresh S. 2025. Revolutionizing clinical laboratories: the impact of artificial intelligence in diagnostics and patient care. *Diag Microbiol Infect Dis*. 111:116728.
12. Land KJ, Boeras DI, Chen X-S, Ramsay AR, Peeling RW. 2019. REASSURED diagnostics to inform disease control strategies, strengthen health systems and improve patient outcomes. *Nat Microbiol*. 4:46–54.
13. Hans L, *et al.* 2021. Early diagnosis of HIV-1 and HIV-2 using cobas HIV-1/HIV-2 qualitative test: a novel qualitative nucleic acid amplification test for plasma, serum, and dried blood spot specimens. *J Acquir Immune Defic Syndr*. 87:1187–1195.
14. Reipold EI, *et al.* 2017. Optimising diagnosis of viraemic hepatitis C infection: the development of a target product profile. *BMC Infect Dis*. 17:707.
15. Piatek AS, Wells WA, Shen KC, Colvin CE. 2019. Realizing the "40 by 2022" commitment from the united nations high-level meeting on the fight to end tuberculosis: what will it take to meet rapid diagnostic testing needs? *Glob Health Sci Pract*. 7: 551–563.
16. Papaiakovou M, Littlewood DTJ, Gasser RB, Anderson RM. 2021. How qPCR complements the WHO roadmap (2021–2030) for soil-transmitted helminths. *Trends Parasitol*. 37: 698–708.
17. Bharadwaj M, Bengtson M, Golverdingen M, Waling L, Dekker C. 2021. Diagnosing point-of-care diagnostics for neglected tropical diseases. *PLoS Negl Trop Dis*. 15:e0009405.
18. World Health Organization. *Global report on neglected tropical diseases 2024*. World Health Organization, 2024.

19. Courtney SJ, Stromberg ZR, Kubicek-Sutherland JZ. 2021. Nucleic acid-based sensing techniques for diagnostics and surveillance of influenza. *Biosensors (Basel)*. 11:47.
20. Allen KE, *et al.* 2018. Survey of diagnostic testing for respiratory syncytial virus (RSV) in adults: infectious disease physician practices and implications for burden estimates. *Diag Microbiol Infect Dis*. 92:206–209.
21. Au WY, Cheung PP-H. 2021. Diagnostic performances of common nucleic acid tests for SARS-CoV-2 in hospitals and clinics: a systematic review and meta-analysis. *Lancet Microbe*. 2:E704–E714.
22. Almasi A, *et al.* 2022. Investigating geographical accessibility and site suitability of medical laboratories in Kermanshah-Iran. *Front Public Health*. 10:1004377.
23. Hønge BL, *et al.* 2013. Loss to follow-up occurs at all stages in the diagnostic and follow-up period among HIV-infected patients in Guinea-Bissau: a 7-year retrospective cohort study. *BMJ Open*. 3:e003499.
24. Bard JD, Babady NE. 2022. The successes and challenges of SARS-CoV-2 molecular testing in the United States. *Clin Lab Med*. 42:147–160.
25. Lakshmanan K, Liu BM. 2025. Impact of point-of-care testing on diagnosis, treatment, and surveillance of vaccine-preventable viral infections. *Diagnostics (Basel)*. 15:123.
26. Kapadia SN, Jordan AE, Eckhardt BJ, Perlman DC. 2024. The urgent need to implement point-of-care RNA testing for hepatitis C virus to support elimination. *Clin Infect Dis*. 78: 1235–1239.
27. Gavina K, Franco LC, Khan H, Lavik J-P, Relich RF. 2023. Molecular point-of-care devices for the diagnosis of infectious diseases in resource-limited settings—a review of the current landscape, technical challenges, and clinical impact. *J Clin Virol*. 169:105613.
28. Boobalan J, *et al.* 2019. Pooled nucleic acid testing strategy for monitoring HIV-1 treatment in resource limited settings. *J Clin Virol*. 117:56–60.
29. Preiser W, van Zyl GU. 2020. Pooled testing: a tool to increase efficiency of infant HIV diagnosis and virological monitoring. *Afr J Lab Med*. 11:1035.
30. Sun H-Y, *et al.* 2022. Three-stage pooled plasma hepatitis C virus RNA testing for the identification of acute HCV infections in at-risk populations. *Microbiol Spectr*. 10:e0243721.
31. Aguilera A, *et al.* 2023. Real-life validation of a sample pooling strategy for screening of hepatitis C. *Clin Microbiol Infect*. 29: 112.E1–112.E4.
32. Cuevas LE, *et al.* 2021. Systematic review of pooling sputum as an efficient tuberculosis testing during COVID-19 pandemic. *Emerg Infect Dis*. 27:719–727.
33. Das S, Frank KM. 2022. Strategies for scaling up SARS-CoV-2 molecular testing capacity. *Clin Lab Med*. 42:261–282.
34. Papaiakovou M, *et al.* 2019. Pooling as a strategy for the timely diagnosis of soil-transmitted helminths in stool: value and reproducibility. *Parasit Vectors*. 12:443.
35. Elsbernd K, *et al.* 2022. Costs and cost-effectiveness of HIV early infant diagnosis in low- and middle-income countries: a scoping review. *Infect Dis Poverty*. 11:82.
36. Wratil PR, *et al.* 2020. Comparative multi-assay evaluation of Determine™ HIV-1/2 Ag/Ab Combo rapid diagnostic tests in acute and chronic HIV infection. *Med Microbiol Immunol*. 209:139–150.
37. Cubas-Atienzar AI, *et al.* 2021. Limit of detection in different metrices of 19 commercially available rapid antigen tests for the detection of SARS-CoV-2. *Sci Rep*. 11:18313.
38. Graham M, *et al.* 2021. Sample pooling on the Cepheid Xpert® Xpress SARS-CoV-2 assay. *Diag Microbiol Infect Dis*. 99: 115238.
39. Cassell MM, Wilcher R, Ramautarsing RA, Phanuphak N, Mastro TD. 2020. Go where the virus is: an HIV micro-epidemic control approach to stop HIV transmission. *Glob Health Sci Pract*. 8:614–625.
40. Cappy P, *et al.* 2022. Effectiveness of the HCV blood screening strategy through eighteen years of surveillance of HCV infection in blood donors in France. *Blood Transfus*. 20:1–7.
41. Vuchas C, *et al.* 2023. Implementation of large-scale pooled testing to increase rapid molecular diagnostic test coverage for tuberculosis: a retrospective evaluation. *Sci Rep*. 13: 15358.
42. Sempos CT, Tian L. 2020. Adjusting coronavirus prevalence estimates for laboratory test kit error. *Am J Epidemiol*. 190: 109–115.
43. Naing L, Nordin RB, Rahman HA, Naing YT. 2022. Sample size calculation for prevalence studies using Scalex and ScalaR calculators. *BMC Med Res Methodol*. 22:209.
44. Schulte PA, *et al.* 2020. Considerations for pooled testing of employees for SARS-CoV-2. *J Occup Environ Med*. 12:1–9.
45. Heidt B, *et al.* 2020. Point of care diagnostics in resource-limited settings: a review of the present and future of PoC in its most needed environment. *Biosensors (Basel)*. 10:133.
46. King BM, Rosopa PJ, Minium EW. *Statistical reasoning in the behavioral sciences.* 7th ed. Wiley, 2011.
47. Funder DC, Ozer DJ. 2019. Evaluating effect size in psychological research: sense and nonsense. *Adv Methods Pract Psychol Sci*. 2:156–168.
48. Benjamin-Chung J, *et al.* 2020. Comparison of multi-parallel qPCR and double-slide Kato-Katz for detection of soil-transmitted helminths infection among children in rural Bangladesh. *PLoS Negl Trop Dis*. 14:e0008087.
49. Rahmani M. 2020. Medical trainees and the Dunning-Kruger effect: what they don't know what they don't know. *J Grad Med Educ*. 12:532–534.
50. Mahumud RA, *et al.* 2016. Diagnostic errors in low and middle-income countries: future health and economic burden for patient safety. *Austin Emerg Med*. 2:id1045.
51. Autor DH. 2024. Applying Ai to Rebuild Middle Class Jobs. *NBER Working Paper No. w*32140 [Preprint]. https://ssrn.com/abstract=4722981 (accessed 2 June 2025).
52. Lee YS, Iizuka T, Eggleston K. 2025. Robots and labor in nursing homes. *Labour Econ*. 92:102666.
53. Rodrigues SM, *et al.* 2022. Digital health-enabled community-centered care: scalable model to empower future community health workers using human-in-the-loop artificial intelligence. *JMIR Form Res*. 6:e29535.
54. Bhamla MS, *et al.* 2017. Hand-powered ultralow-cost paper centrifuge. *Nat Biomed Eng*. 1:0009.
55. Márquez-Islas R, Pérez-Pacheco A, Quispe-Siccha R, Salazar-Nieva LB, García-Valenzuela A. 2022. Visual assessment of blood plasma versus optical transmittance and refractive index measurements for quantifying lipemia. *Diagn*. 12:510.

56. Sakundarno M, *et al.* 2009. Insufficient quality of sputum submitted for tuberculosis diagnosis and associated factors, in Klaten district, Indonesia. *BMC Pulm Med*. 9:16.
57. Britt-Rodriguez K, Daniel J, Hayden J. 2024. Surreptitious pipetting errors on a vendor-programmed liquid handler. *J Mass Spectrom Adv Clin Lab*. 33:1–3.
58. Velasco PQ, *et al.* 2024. Optimization of liquid handling parameters for viscous liquid transfers with pipetting robots, a "sticky situation". *Digit Discov*. 3:1011–1020.
59. Tegally H, San JE, Giandhari J, Oliveira T. 2020. Unlocking the efficiency of genomics laboratories with robotic liquid-handling. *BMC Genomics*. 21:729.